Biolubrication enhancement for tissues and biomaterials

Wan, Hongping

DOI:
10.33612/diss.135598825

Chapter 4

A bioinspired mucoadhesive restores lubrication of degraded cartilage through reestablishment of lamina splendens

Hongping Wan, Ke Ren, Hans J. Kaper, Prashant K. Sharma
Colloids and Surfaces B: Biointerfaces, 2020, 193; 1109773

Abstract

Adsorbed lubricious films composed of biomacromolecules are natively present at all articulating interfaces in the human body where they provide ultralow friction and maintain normal physiological function. Biolubrication gets impaired due to diseases such as osteoarthritis, in which cartilage damage results from alterations in synovial fluid and lamina splendens composition. Osteoarthritis is treated with hyaluronic acid (HA) orally or via intra-articular injection, but due to the poor adsorption of HA on the cartilage surface in the absence of adhesive molecules, pain relief is temporary. Here, we describe how natural lubrication on degraded cartilage surface can be restored with the help of a bioinspired mucoadhesive biopolymer chitosan catechol (Chi-C). Quartz crystal microbalance was used to mimic the formation of lamina splendens in vitro, known as synovial fluid conditioning films (SyCF), and atomic force microscopy was used to measure their nanoscale frictional properties. Clear evidence of glycoprotein (PRG4) recruitment by Chi-C increased the softness of SyCF, which also improved nanoscale lubrication *in vitro*, decreasing the friction coefficient from 0.06 to 0.03. At the macroscale, cartilage damage induced by Chondroitinase ABC increased the coefficient of friction (COF) from 0.07 ± 0.04 (healthy tissue) to 0.15 ± 0.03 (after tissue damage) in the presence of synovial fluid after sliding for 50 minutes. After Chi-C treatment of damaged cartilage, the COF fell to 0.06 ± 0.03, which is comparable to healthy cartilage. Chi-C did not adversely affect the metabolic activity of human chondrocytes. This study provides new key insight into the potential for restoring biolubrication through the use of muco-adhesive molecules.

Keywords: cartilage lubrication; chitosan; catechol; lamina splendens; biolubrication

1.Introduction

Lubrication mediated by adsorbed biomacromolecules (proteins, glycoproteins and polysaccharides) is vital for the active function of tissues and implants, especially at sliding interfaces, like tongue-enamel [1], tongue-mucosa, cornea-eye lid [2], cartilage-cartilage or cartilage-meniscus [3] interfaces. These biomacromolecules are secreted by exocrine glands such as the lacrimal and salivary glands, or by specialized cells like chondrocytes present in cartilage. The secreted biomacromolecules form a lubricious film on articulating surfaces, which yields low friction under high stress and efficiently maintains physiological function. In the articular joints, for instance, the dynamic friction coefficient of hyaline cartilage lubricated with synovial fluid (SF) is extremely low (μ~0.005) [3]. The exact mechanism underlying joint and cartilage lubrication is still subject to debate. Lamina splendens which is an acellular and non-fibrous layer [4] adsorbed on parallelly-oriented collagen fibrils at the surface of the cartilage is held responsible for this super lubricity (μ~0.005) [3]. Lamina splendens [5] is composed of hyaluronan (HA), lubricin also called proteoglycan 4 (PRG4), surface active phospholipids and other proteins, which work synergistically yielding high lubrication [6,7].

Old age, injury or diseases like arthritis cause alterations in the composition of SF and lamina splendens, leading to lubrication dysfunction. Alterations in the synovial fluid (SF) composition due to the decreased molecular weight of HA caused by enzymatic cleavage [8] is associated with an aberrance in the adsorbed film, resulting in decreased viscosity and lubrication. To restore the viscosity, HA is administered orally or through viscosupplementation, in which a highly viscous solution of HA is injected in the synovial cavity for pain relief. Exogenous HA has been shown to have lubrication, anti-inflammatory and chondroprotective functions [9], but in the clinical setting multiple injections are necessary, and the pain relief is temporary [10,11] due to the poor adhesion and clearance of exogeneous HA from the joint cavity [12]. Specific HA binding peptide [13] has been used to increase adsorption of HA on the cartilage surface, which yielded better lubrication. Exogeneous lubricating molecules e.g. tissue-reactive polyoxazoline graft-copolymers [14] or biomimetic diblock copolymer [15] have also shown to restore cartilage lubrication. But in an actual damaged joint

cavity with limited SF, PRG4 is are still endogenously available in abundance. This component have excellent boundary lubricating properties [16] and could potentially be utilized as part of treatment instead of being disregarded.

Intrigued by studies showing that cationic polyelectrolytes, especially the mussel-inspired biopolymer [17], can improve the mechanical strength of polysaccharide multilayers, we tested their ability to act as an additive during viscosupplementation to improve cartilage lubrication by enhancing the lamina splendens. To investigate its potential to restore cartilage lubrication, in the present study we chose chitosan-catechol (Chi-C), a bioinspired, biocompatible and inexpensive molecule with long-lasting mucoadhesive properties [18]. Chitosan is characterized by its mucoadhesive properties with strong electrostatic interaction and its large amount of hydrogen bonding. In particular, modification of chitosan with catechol makes it water-soluble at neutral pH [18], and its oxidized derivative can bioconjugate with amines and cysteine residues of protein or glycoprotein through the Michael addition or Schiff bases formation [19]. Degraded cartilage remains predominantly negatively charged, and collagen fibrils, containing amine and carboxyl groups, would be exposed.

We hypothesize that Chi-C binds to and absorbs on the exposed collagen fibrils of degraded cartilage and other proteinaceous constituents of the lamina splendens. Sessile Chi-C then attracts and recruits lubricin (PRG4) from the SF and reestablishes and strengthens the lamina splendens. We tested the above hypothesis using Chi-C with a conjugation degree of 12.7%. The kinetics of the formation of lamina splendens *in vitro* hereinafter called the synovial fluid conditioning films (SyCF), and its modification with Chi-C was monitored using a quartz crystal microbalance with dissipation QCM-D. Alteration in SyCF composition was monitored using X-ray photoelectron spectroscopy (XPS) and fluorescent Concanavalin A (ConA) staining. The lubrication properties at nanoscale were measured by colloidal probe AFM. To demonstrate whether this concept works at the macro-scale, an *ex vivo* friction system was used, which was based on enzymatically (Chondroitinase ABC) degraded cartilage. Finally, the safety of Chi-C use was demonstrated through the proliferation and metabolic activity of chondrocytes.

2. Materials and methods

2.1. Synthesis of chitosan-catechol (Chi-C)

Chi-C was synthesized through the EDC reaction between the carboxyl group from hydrocaffeic acid and the amine group from chitosan [20] at pH 5 (**Figure S1**). The success of conjugation was proven using ^{1}H-NMR and conjugation degree was assessed using Uv-Vis spectrophotometer. The method in detail is described in the supplementary information.

2.2. Synovial fluid and cartilage collection

Bovine synovial fluid was aspirated from bovine (2-year-old bulls) stifle joints within 2 hours of slaughter. The stifle joints were obtained from a local slaughterhouse (Kroon Vlees b.v., Groningen, the Netherlands). The muscles and flesh surrounding the knee joint were cut carefully to reach the areas where most of the synovial fluid was present. The fluid was collected with an 18G spinal needle from 3 different joints and pooled. The total amount of fluid was centrifuged at 1500 rpm for 5 minutes to separate out cells and then divided into aliquots of 1.5 mL and stored immediately at -80 ^{0}C for further use. On average, 5 ml of synovial fluid was aspirated from each knee joint. Bovine synovial fluid was used because its lubricating properties are similar to human synovial fluid [21]. The femoral condyle bovine cartilage was extracted from bovine knees with a bone thickness of 5mm and a surface area of 40×25 mm^2 by sawing. The cartilage was then mounted to the bottom component of the universal mechanical tester (UMT). After this, a plug 9 mm in diameter was drilled out of the tibial plateau [22], extensively washed with PBS and mounted to the top component on the load cell of the UMT.

2.3. Quartz crystal microbalance with dissipation (QCM-D) to monitor the role of Chi-C in modifying the synovial fluid condition films

QCM-D device model Q-sense E4 (Q-sense, Gothenburg, Sweden) was used to study the formation of synovial fluid condition film (SyCF) and its interaction between Chi-C. The gold-coated, AT-cut quartz crystals, with a sensitivity of 17.7 ng cm^{-2} for a 5 MHz sensor crystal, were used as substrates. At the start of an experiment, the crystal was cleaned by UV/ozone treatment for 10 min and then washed by a mixture solution of ultrapure-water, ammonium hydroxide,

and H_2O_2 (v:v:v 3:1:1) at 75°C for 10 min, followed by another 10 min of washing with ultrapure-water and finally dried by N_2 and another 10 min of UV/ozone treatment. The crystals were mounted on the crystal holders and placed in the E4 unit of the QCM-D. The crystals were excited in air at 5 MHz and to their 13^{th} overtone to check for any mounting errors. The chamber above the QCM crystal was then perfused with 10 mM PBS using a peristaltic pump (Ismatec SA, Switzerland) until the stable baselines of frequency and dissipation were achieved. In order to mimic the *in vivo* situation, the synovial fluid was perfused with a flow rate of 50µl/min, corresponding with a shear rate of 3 s^{-1}, at 25°C for 30 min to form the synovial fluid conditioning film (SyCF) on top of the QCM-D crystal. Then the chamber was sequentially perfused with 0.05% w/v solution of Chi-C in PBS for 10 min and followed by another 30 min of synovial fluid flow to form a layer-by-layer secondary SyCF (S-SyCF). Between each step, the chamber was perfused with buffer for 10min to remove unattached or loosely adhering molecules from the tubing, chamber and the crystal surface. Frequency (Δf) and dissipation (ΔD) shifts were measured in real-time during perfusion to monitor the kinetics, where the $\Delta D/\Delta f$ ratio was the indicator of the layer softness. After experiments, crystals were carefully removed from the QCM-D and immediately used for further experiments while keeping them hydrated the whole time. To get the negative control of S-SyCF the intermediate exposure of Chi-C was replaced with just a buffer rinse.

2.4. Surface composition analysis by X-ray photoelectron spectroscopy (XPS)[23]

The elemental composition of the layer surface was detected by XPS (S-Probe, surface science instruments, Mountain View, CA, USA); XPS can only detect the elemental composition of a sample from the top 10 nm thick surface. First, S-SyCF adsorbed on Au-coated crystal was air- dried and then moved to XPS pre-vacuum chamber with a pressure of 10^{-7} Pa. X-rays (10KV, 22mA) with a spot size of 250×1000 um, were produced using an aluminum anode. Binding energy spectra with a range of 1-1100 eV were made at low resolution and corrected with sensitivity factors provided by the manufacturer. The area under each peak yielded elemental surface concentrations in percent. The

fraction of O_{1S} peak at 532.7eV (% $O_{532.7}$) from carboxyl groups [24] was used to calculate the amount of oxygen present in the glycosylated moieties, i.e. PRG4 amount (%O_{glyco}).

$$\%O_{glyco} = \%O_{532.7} * \%O_{total} \quad (3)$$

Where %O_{total} is the total percentage of oxygen.

2.5. Glycoprotein visualization using Concanavalin A (ConA) stain

ConA is widely used to stain the glycoproteins and mucins [25]. After the QCM-D experiment, the crystal was removed and fixed with 4% paraformaldehyde (Sigma, CAS no.30525-89-4) at room temperature for 30 min. After washing with PBS 3 times (15 min), Alexa Fluor™ 488 Conjugate of Concanavalin A (ThermoFisher, Catalog no. C11252) with a concentration of 1µg/ml in PBS was added on top of the crystal surface and incubated at room temperature for 45 min. The crystal surface was rinsed 3 times by dipping in PBS for 5 minutes each time, and then fluorescent images were made using a confocal microscope (TCS SP2, Leica, Wetzlar, Germany) equipped with an argon ion laser at 488 nm. The crystal was always kept wet and in the dark during staining and before microscopic examination. The green fluorescent intensity from each fluorescent micrograph was calculated using Image J software [26].

2.6. Colloidal probe atomic force microscopy for studying lubrication at the nanoscale [24]

The lubrication properties and the surface topography of S-SyCF were evaluated using the atomic force microscopy (Nanoscope IV Dimension^{tm} 3100, USA). Friction force was measured using a colloid probe equipped with a Dimension Hybrid XYZ SPM scanner head (Veeco, New York, USA) on the S-SyCF, with and without Chi-C treatment. Detailed protocol is presented in the supplementary information.

2.7. Cartilage degradation and lubrication properties in an *ex-vivo* cartilage-cartilage friction system

Freshly obtained pieces of cartilage were immersed in one unit of chondroitinase ABC (ChABC) pre-dissolved in 0.01% bovine serum albumin solution in PBS (BSA/PBS) at 37°C for 1 h [14]. Control samples were immersed in 0.01% BSA/PBS for the same period time and temperature. Both the healthy

cartilage and degraded cartilage were analyzed by histology as follows. Pieces of cartilage (5 × 5 × 4 mm^3) were decalcified with 10% EDTA (Sigma ED2SS, CAS 6381-92-6) solution for 6 weeks and every 3 days the solution was changed. After decalcification, the pieces of cartilage were washed 3 times with PBS (30 min per wash) and with demi water for 10 min. The cartilage was then dehydrated with 50% alcohol (1× 60 min), 70% alcohol (1×60 min), 96% alcohol (1×60 min), 100% alcohol (3×60 min) followed with xylene (3× 60 min) and finally embedded in paraffin. Cartilage sections were cut into 5 µm thickness by a cryostat (Cryostar NX70, Thermo Scientific) and stained by w/v 0.5% Fast Green for 5 min followed with 1% acetic acid dip, another 5min Safranine-O (0.1%) staining, were then visualized under the microscope. The collagen networks were stained with the picrosirius red [27] (Direct Red 80, 0.1% solution in picric acid) for 60 min and visualized under the microscope. The healthy or degraded cartilage extracted from bovine knees with 5 mm bone thickness and a surface area of 40mm×25mm were mounted to the bottom component of a UMT (UMT-3, CETR Inc., USA).

Cartilage pairs [22] of healthy and degraded cartilage were mounted to the UMT3 as shown in Figure 4. The plug-tibial plateau interface was submerged in 500µl bovine synovial fluid (SF) to make sure that the surfaces were covered with fluid, thus mimicking the physiological situation during reciprocation sliding. Several plug-tibial plateau pairs of degraded cartilage were pre-incubated in Chi-C (0.5mg/ml in PBS) for 10 min before being submerged in SF. A force of 4N [22] was applied during reciprocation sliding at a sliding velocity of 4 mm/s and sliding distance of 10 mm per cycle for 50 minutes. All cartilage friction experiments were performed at 35°C to mimic the physiological temperature in the knee joint.

2.8. Evaluation of cell behavior

Cell response to Chi-C treated S-SyCF was tested using an XTT assay (Applichem A8088) on chondrocytes derived from human cartilage [28] using a protocol described in detail in the supplementary information.

2.9. Statistical analysis. All data are expressed as means ± SD. Differences between groups determined with a two-tailed Student's t-test, with significance set at $p < 0.05$.

3. Results and Discussion

3.1. Synthesis and characterization of chitosan catechol (Chi-C) polymer

In the present study, we chose 12.7% catechol conjugation for the used Chi-C as a proof of principle. Detailed characterization of the Chi-C using 1H-NMR and UV-Vis spectroscopy are available in the supplementary information. The zeta potential of Chi-C measured at a concentration of 0.5mg/ml in PBS is 7.65±1.5 mV, taking a small positive charge as showing in **Figure S2**.

3.2. Effect of Chi-C on the softness and composition of synovial fluid conditioning films

3.2.1 Kinetics of synovial fluid conditioning film (SyCF) formation and Chi-C adsorption

Lamina splendens is composed of various biomacromolecules such as HA, PRG4 and lipids, which coat the cartilage surface and remain in equilibrium with the synovial fluid. Any removal or degradation would be replenished by the synovial fluid (SF). This layer was mimicked *in vitro* by allowing adsorption of SF macromolecules onto the Au coated QCM crystal. The substrate properties i.e. hydrophilicity and charge is shown to affect the adsorption and lubrication behavior of lubricin [29]. Thus we have chosen Au [30], which is hydrophilic with negative charge and would mimic the cartilage with collagen type II interlaced with aggrecan molecules. Adsorption from the SF gave rise to a synovial fluid condition film (SyCF) with a frequency shift for the third overtone (Δf_3) of -70±5 Hz and a dissipation (ΔD_3) change of 10^{-5}, indicating a large amount of protein adsorption on the top of QCM crystal surface (**Figure 1**). The $-\Delta D_3/\Delta f_3$ ratio of larger than 10^{-6} indicates the formation of a very soft and hydrated SyCF [24,31]. Exposure of SyCF to Chi-C (0.5mg/ml) gave rise to a very large frequency and dissipation shifts (**Figure 1b,c**), which did not occur when the SyCF was exposed to PBS alone (**Figure 1a,c**), thus indicating a high affinity between Chi-C and SyCF. Although slightly decreased in structural softness of SyCF ($-\Delta D_3/\Delta f_3$) after Chi-C treatment due to the electrostatic force

or covalent binding no significant difference was observed compared to SyCF exposure to PBS (**Figure 1d**).

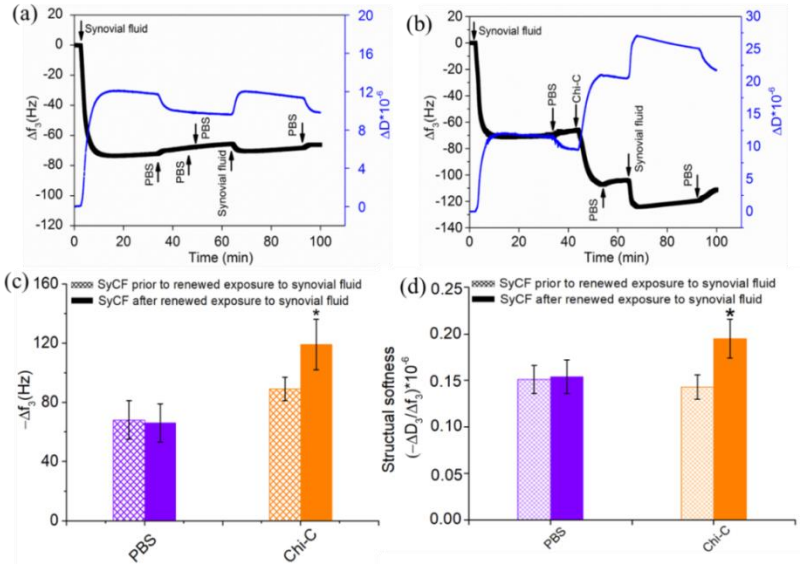

Figure 1. Quartz crystal microbalance with dissipation curves showing the kinetics of SyCF formation with or without (PBS) exposure to Chi-C and reflow of synovial fluid, which causes formation of a top layer (S-SyCF) with high structural softness. Frequency and dissipation shifts for the SyCF, (a) buffer or (b) Chi-$C_{12.7\%}$ treatment and reflow of SF for the formation of S-SyCF. (c) Frequency shift before and renewed exposure to SF with treatment of PBS and Chi-C. (d) Structural softness of the SyCF with prior exposure to PBS or Chi-C and after renewed exposure to SF. Error bars represent the standard deviation over three independent measurements. *Statistically significant ($p<0.05$) (two tailed Student t-test) differences in softness and frequency compared to control film.

The renewed flow of SF gave rise to further shifts (**Figure 1b,d**) on Chi-C exposed to SyCF, where an even higher $-\Delta D_3/\Delta f_3$ was observed. This indicates a further increase in softness of the S-SyCF. This can happen if Chi-C that is bound to the SyCF recruits additional large and hydrated molecules from the SF on the surface, leading to an increase in softness. On the PBS exposed SyCF, no obvious changes (**Figure 1a**) were observed in frequency or dissipation. No significant difference was observed in structural softness of SyCF after Chi-C and PBS treatment, which could be due to the low positive charge of Chi-C (7.65±1.5 mV) that could cause its adsorption on SyCF but insufficient to

change the structural softness. This observation is opposite to the supercharged proteins [24] which caused rigidification of salivary condition films upon interaction. Chi-C can still recruit macromolecules from SF and finally yield a much softer S-SyCF.

In SF, large amounts of molecules such as PRG4, HA, lipids and proteins have a negative charge in the physiological environment [32,33] and adsorb on the surface to give rise to the SyCF. Chi-C has a positive charge and can electrostatically interact with the SyCF. Moreover, SyCF is full of amine residues, which readily combine with catechol-oxidized derivative via Michael addition or Schiff bases formation in the physiological environment [34]. Chi-C adsorption on the SyCF could therefore be caused by electrostatic interactions as well as chemical consolidation between Chi-C and the synovial fluid molecules. Similar electrostatic and chemical bonding is expected to take place between the sessile Chi-C and SF molecules upon reflow of SF to form the S-SyCF. We therefore postulate that Chi-C strongly adsorbs on the SyCF and then recruits large highly hydrated negatively charged molecules like HA, albumin and glycoprotein (shown by the increased softness) from the SF.

3.2.2. Change in surface composition of S-SyCF due to exposure to Chi-C

S-SyCF surface composition was determined using high-resolution X-ray photoelectron spectroscopy. Full peak description is presented in **Table S1**, which shows that the relative content of C, O and N changes upon exposure to Chi-C. The C_{1s} peak of each surface could be deconvoluted into three different peaks: C–(C,H), C–N/C–O, and C=O/O-C-O; their percentages for S-SyCF with PBS and Chi-C exposure is different, as shown in **Figure 2a** and **Table 1**, suggesting different protein content on these surfaces. For S-SyCF with Chi-C, the relative content of C-C binding (**Table 1**) and P (**Table S1**) were slightly increased, which may be attributed to the lipid adsorption whose acyl chain contain C-C binding and P in the dipolar head groups [35]. The O_{1s} peak could be deconvoluted into two components: O=C-N and C-O-H, which is considered to be the O from the protein and glycol group, respectively. The relative content of glycoprotein [24] was calculated with the O_{1s} peak area at 532.7ev (Figure 2b). The peak area (532.7ev) for S-SyCF formed with Chi-C exposure was 5.86±0.25, which is significantly higher than the value of 4.8±0.3 for S-SyCF formed with

PBS exposure. This indicates that Chi-C recruited glycoproteins and lipids from the SF on the SyCF surface.

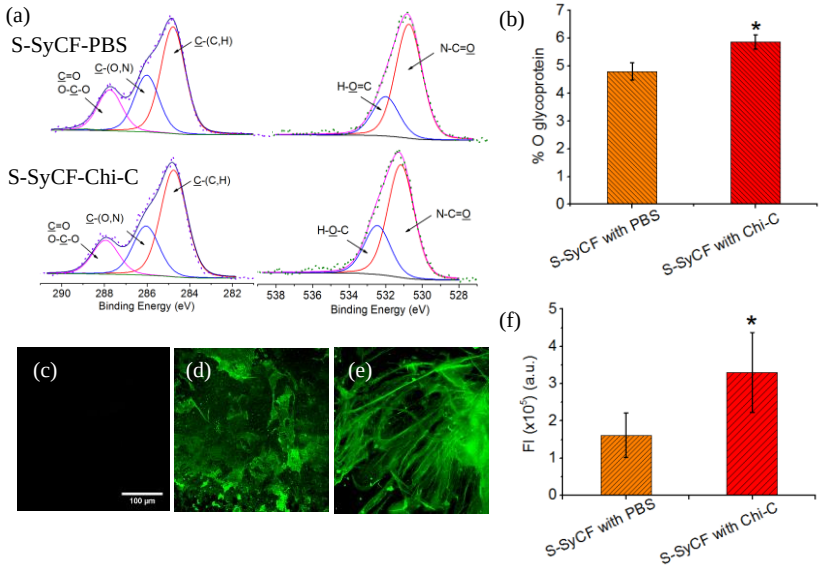

Figure 2. Difference in Surface composition of the S-SyCF formed after intermediate exposure to buffer or Chi-C. (a) XPS analysis with decomposed C and O peaks of S-SyCF layer with PBS and Chi-C treatment. (b) The degrees of glycosylation (%O glycoprotein) of synovial fluid without adsorbed Chi-C and with adsorbed Chi-C were obtained from a decomposition of the O_{1s} photoelectron peak in XPS. Error bars represent the standard deviations over three independent XPS measurements. (c) ConA staining of bare crystal, (d) S-SyCF with buffer and (e) S-SyCF with Chi-C exposure. (f) Statistically significant ($p < 0.05$, two tailed Student t-test) difference between S-SyCF layer with PBS and Chi-C.

ConA-alexa staining of bare crystal did not show any fluorescent emission (**Figure 2c**). Both the surfaces with S-SyCF (**Figure 2d,e**) showed green fluorescence, a stronger green fluorescence was detected for S-SyCF exposed to Chi-C (**Figure 2e,f**) as compared to buffer exposure (**Figure 2d,f**), indicating higher glycoprotein binding on the SyCF exposed to Chi-C. The fluorescence results agree with the XPS results.

Based on the *in vitro* fluorescence, XPS and the QCM-D results, it is clear that Chi-C readily adsorbs to the SyCF. Furthermore, sessile Chi-C recruits glycoproteins (PRG4) to give rise to a very soft and hydrated S-SyCF. We

therefore expect that Chi-C would adsorb on intact or degraded lamina splendens *in vivo*. Locations on damaged cartilage completely devoid of the lamina splendens would expose the collagen type II fibrils containing 141 negatively charged amino acids [36] and the proteoglycan [37], which is negatively charged and abundant in amine groups. Chi-C can also have electrostatic and chemical interactions with collagen fibrils. Sessile Chi-C shows a tendency to recruit PRG4 and lipid from the SF, which would cause restoration of damaged lamina splendens and its reestablishment on exposed collagen fibrils.

Table 1. Surface chemical bonding of SF with PBS and SF with Chi-C

Samples	C_{1s} BE and relative area (%)			O_{1s} BE and relative area (%)	
	C-C	C-N	C=O	N-C=O	H-O-C
SF with PBS	50.6	30.1	19.3	74.1	25.9
SF with Chi-C	52.0	27.3	20.7	70.5	29.5

3.3 Nano-scale lubrication properties of S-SyCF

On the bare sensor surface, the F_f increased linearly with F_n, corresponding to a high COF of 0.27 ± 0.04 (**Figure 3a**). On S-SyCF exposed to buffer, the COF decreased to 0.06 ± 0.005, which was attributed to the lubricious macromolecules in synovial fluid such as HA, lipids and PRG4 [38]. When S-SyCF was exposed to Chi-C, a further decrease in COF to 0.03 ± 0.006 occurred. This extremely low COF can be attributed to its higher structural softness because Chi-C recruited larger amounts of glycoproteins (PRG4) from synovial fluid. For salivary condition films, previous research showed that increased structural softness leads to lower COF at nanoscale [24]. Contact of the AFM colloid probe with the bare sensor surface showed very little repulsive forces indicating a hard material surface. SyCF coated crystal surfaces showed a long-range repulsive forces (**Figure 3b**). When exposed to Chi-C, S-SyCF showed longer range repulsive forces as compared to PBS exposed.

The topography of S-SyCFs was investigated using a sharp tip on AFM, as shown in Figure 3c. Bare sensor crystals had a smooth surface, while S-SyCF presented uneven, globular structures due to adsorption of synovial lubricant with heights of about 22 ± 5 nm. Numerous similar structures were observed with a height of 33 ± 8nm for S-SyCF exposed to Chi-C.

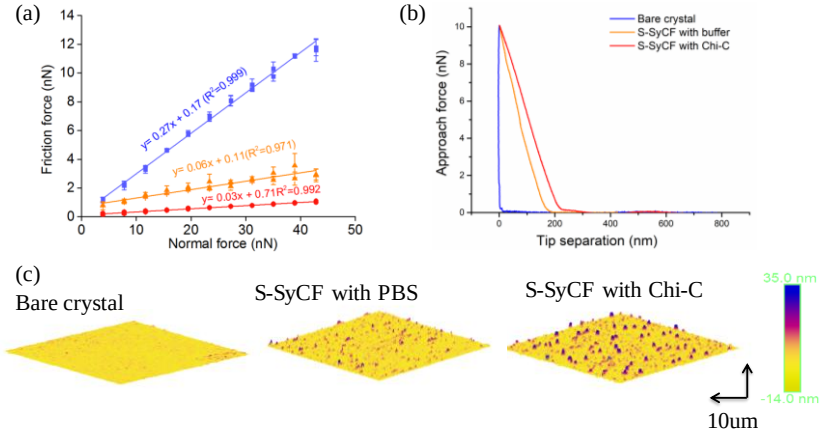

Figure 3. Morphology, topography and nano-frictional properties of S-SyCF with intermediate exposure to either buffer or Chi-C. (a) Friction force as a function of normal force during increasing and decreasing normal forces represent the COF of each layer calculated by the slope of the linear fitting line. Error bars represent standard deviations over 3 friction loop measurements. (b) Example of the repulsive force as a function of tip separation distance for bare Au-coated QCM crystals, SF film on crystal and SF with Chi-C on crystal.

The results from QCM-D, XPS, ConA staining and AFM clearly show that Chi-C exposure not only stabilizes the SF film through physical and chemical interactions, but also enables it to recruit glycoproteins (PRG4) from the synovial fluid to create a softer layer, which enhances the boundary lubrication measured using AFM.

3.4. *Ex-vivo* degraded cartilage friction system to characterize the effect of Chi-C treatment on lubrication.

After Chondroitinase ABC (ChABC) degradation, a substantial reduction of GAGs was observed compared to the cartilage without degradation(shown in **FigureS3**). In contrast, the collagen structure remained unmodified, and no differences could be detected between the healthy cartilage and degraded cartilage. Our findings on ChABC for cartilage degradation are consistent with a previous study reporting that ChABC degraded the GAGs rather than collagen [14]. Comparing these histological data with the reference [14] and the description of OA [39], it appears that ChABC treatment mimics the early stage (I or II) of OA. We used UMT3 to test the tribological performance of degraded cartilage with

or without Chi-C treatment. Figure4a shows how the COF changed from the first sliding cycle to 50 minutes of sliding. For healthy cartilage (positive control) the COF remained stable at around 0.07 ± 0.04 for 50 minutes. For degraded cartilage (negative control) the COF gradually increased to 0.15 ± 0.03 during 50 minutes (**Figure 4a**), which is significantly higher than healthy cartilage. Morgese et al. [14] also reported a similar increase in COF for cartilage degraded with ChABC. Without the protection of the superficial layer, and with insufficient boundary lubrication, the friction force increased gradually. For degraded cartilage that was pre-exposed to Chi-C (0.5mg/ml in PBS) for 10 min, the COF remained low (0.06 ± 0.03) for the 50 minutes test cycle. No statistically significant difference was found compared to healthy cartilage (**Figure 4a**). The COF at the end of 50 minutes of sliding was significantly lower ($P<0.05$) for Chi-C-treated degraded cartilage than for degraded cartilage without Chi-C treatment (both measured in SF). Since cartilage is a kind of viscoelastic nonlinear material, the energy dissipation would naturally occur during the reciprocating sliding behavior [40], which has been shown to be directly correlated with the damage of the soft tissue. The energy dissipation increases gradually with time, especially between the degraded cartilages in **Figure4b**: their energy dissipation is higher than the healthy cartilage and degraded cartilage treated with Chi-C. The higher energy dissipation observed on the degraded cartilage could be caused by the unprotected GAGs on cartilage after ChABC treatment, leading to insufficient lubrication and high friction. The COF was measured at 4N of normal load, which mimics the contact pressures in the swing phase of the gait cycle. Previous *ex vivo* experiments [22] have shown that this load does not initiate fluid weeping from the cartilage and thus cannot give rise to formation of a fluid film. In the absence of a fluid film, most of the load is supported through cartilage-cartilage contact, where boundary lubrication takes place predominantly. The COF of degraded cartilage and healthy cartilage observed in the present study is consistent with a previous study [14] that reported a COF of 0.14 for degraded cartilage and 0.06 for healthy cartilage with a similar *ex-vivo* model.

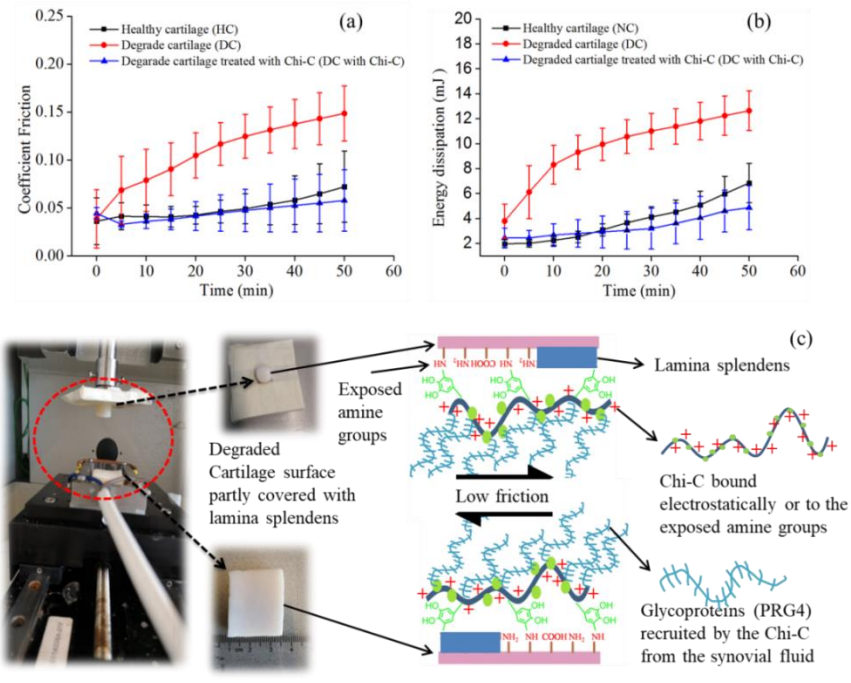

Figure 4. Role of Chi-C in *ex-vivo* friction of degraded cartilage in synovial fluid. (a) Coefficient of friction as a function of time for healthy, degraded and Chi-C-treated (10 min) degraded cartilage submerged in synovial fluid. (b) Friction energy dissipation with time under constant load force (4N). (c) Schematic figure of degraded cartilage reciprocating sliding against another degraded cartilage on the UMT-3, where bottom cartilage is 40×25 mm^2, and the top has a diameter of 9 mm. Degraded cartilage is partly covered with lamina splendens and Chi-C interacts with the surface in turn recruits glycoproteins (PRG4) from the synovial fluid and provides low friction.

Our results and those from Sun et al. [15], Singh et al. [13] and Morgese et. al. [14] show that cartilage lubrication enhancement is possible through immobilization (covalently or non-covalently) of a layer composed of either exogenous lubricious molecules [14,15] or intermediate molecules [13] that recruit lubrication moieties from the SF on the cartilage surface. Morgese et al. [14] used exogenous polyoxazoline graft-copolymers and Sun et al. [15] used biomimetic diblock copolymer that could bind to degraded cartilage, suggesting that the film on the cartilage surface is responsible for boundary lubrication. Singh et al. [13] used HA binding peptides to specifically bind and immobilize HA to the surface of degraded cartilage, suggesting that a high concentration of HA in the

synovial cavity alone is not enough to enhance lubrication, but that HA adsorption on the degraded cartilage surface is necessary. Our strategy is similar to that of Singh et al. [13], whereby the added molecules act as an intermediator between the cartilage surface and lubricious moieties from the SF: PRG4 in our study and HA in the study by of Singh et al. [13]. The difference is that Chi-C does not have any specific PRG4 binding ability, but simply works through physical and chemical attraction and albumin, abundantly present in SF, does not seem to block the interactions [41]. Looking at the commercial aspects, Chi-C is an easier molecule to synthesize in large quantities without being expensive as compared to the HA binding peptide, biomimetic diblock copolymer and polyoxazoline graft-copolymers, in our opinion. We have shown that Chi-C can be effective in a complex situation where synovial fluid, composed of various proteins, polysaccharides, glycoproteins and lipids, is naturally present. One limitation for the use of Chi-C could be the patients suffering from shellfish allergy [42]. But is such cases chitosan from the fungal source [43] can be used for the synthesis of Chi-C instead of marine chitosan.

AFM mimics boundary lubrication conditions at nanoscale and *in vitro*. In the present study, we measured friction on mimicked lamina splendens, i.e. the S-SyCF, whereby Chi-C treatment reduced COF on the AFM by half: from 0.06 to 0.03 (**Figure 3a**). *Ex-vivo* measurements on degraded cartilage showed a similar reduction of COF by half: 0.15 to 0.06 (**Figure 4**). However, the exact COF values remained different. This could be due to the use of different tribo-pairs, i.e. real cartilage vs. QCM crystal surface. Furthermore, frictional properties are often different at nanoscale and macroscale [44]. The *ex vivo* results together with nanoscale friction (AFM), QCM-D, XPS and ConA staining results indicate that Chi-C would readily adsorb on both healthy and degraded cartilage surfaces. We have shown strong evidence that sessile Chi-C recruits glycoproteins (PRG4) from the SF on the cartilage surface, consolidating the lamina splendens and restoring lubrication. Chi-C is a mucoadhesive and it would preferably recruit glycoproteins but hyaluronan (HA) and lipids may also adsorb on the Chi-C treated cartilage surface. HA and lipid adsorption will further consolidate the lamina splendens and enhance lubrication due to the synergistic effect of hyaluronan, glycoprotein and lipids [6]. Intra-articular

delivery of Chi-C alongside HA would not only increase the viscosity of the SF, but also create a condition in which the lamina splendens could be restored with the help of glycoproteins from the patient's own SF and protect the degraded cartilage surface from further degradation.

3.5. Tissue-friendly nature of Chi-C

Both microscopic examination of chondrocytes and XTT assay showed that S-SyCF with Chi-C treatment enables human chondrocyte cells to be as active metabolically and to proliferate and spread as rapidly as S-SyCF with buffer treatment. Detailed description of results are available in the supplementary information including **Figure S4**.

4. Conclusions

We have demonstrated that Chi-C binds to lamina splendens and in turn enhances the boundary lubrication on the degraded cartilage surface through recruitment of glycoproteins (PRG4) from the synovial fluid. This enhancement results in reduction of friction both *in vitro* at nanoscale and *ex vivo* between degraded cartilage surfaces at macroscale. This makes Chi-C, a simple, inexpensive, bioinspired and biocompatible mucoadhesive as a promising additive to the intraarticular viscosupplementation fluid. A proof of principle for cartilage lubrication is obtained, but similar recruitment mechanisms may be applied to sliding tissue-tissue or tissue-biomaterial interfaces in the human body.

Acknowledgements

The UMT-3 tribometer (Bruker) setup was purchased with funding provided by grant no. 91112026 from the Netherlands Organization for Health Research and Development (ZonMW). We also would like to thank the China Scholarship Council for providing a 4-year scholarship to enable Drs. H. Wan to pursue her PhD studies.

References

(1) Vinke, J.; Kaper, H. J.; Vissink, A.; Sharma, P. K. Sci. Rep. 2018, 8 (1), 9087.
(2) Vehof, J.; Sillevis Smitt-Kamminga, N.; Kozareva, D.; Nibourg, S. A.; Hammond, C. J. Am. J. Ophthalmol. 2016, 162, 59–64.
(3) Seror, J.; Zhu, L.; Goldberg, R.; Day, A. J.; Klein, J. Nat. Commun. 2015, 6, 6497.
(4) Athanasiou, K. A.; Darling, E. M.; DuRaine, G. D.; Hu, J. C.; Reddi, A. H. Articular cartilage, Second Edi.; Second, Ed.; CRC Press: Boca Raton, FL, 2017.
(5) Rexwinkle, J. T.; Hunt, H. K.; Pfeiffer, F. M. Front. Mech. Eng. 2017, 12 (2), 234–252.
(6) Jahn, S.; Seror, J.; Klein, J. Annu. Rev. Biomed. Eng. 2016, 18 (1), 235–258.
(7) Pradal, C.; Yakubov, G. E.; Williams, M. A. K.; McGuckin, M. A.; Stokes, J. R. Bioinspiration and Biomimetics 2019, 14 (5).
(8) Kosinska, M. K.; Ludwig, T. E.; Liebisch, G.; Zhang, R.; Siebert, H. C.; Wilhelm, J.; Kaesser, U.; Dettmeyer, R. B.; Klein, H.; Ishaque, B.; Rickert, M.; Schmitz, G.; Schmidt, T. A.; Steinmeyer, J. PLoS One 2015, 10 (5), 1–18.
(9) Webb, D.; Naidoo, P. Orthop. Res. Rev. 2018, 10, 73–81.
(10) Campbell, K. A.; Erickson, B. J.; Saltzman, B. M.; Mascarenhas, R.; Bach, B. R.; Cole, B. J.; Verma, N. N. Arthrosc. J. Arthrosc. Relat. Surg. 2015, 31 (10), 2036-2045.e14.
(11) Maheu, E.; Rannou, F.; Reginster, J.-Y. Semin. Arthritis Rheum. 2016, 45 (4), S28–S33.
(12) Tadmor, R.; Chen, N.; Israelachvili, J. N. J. Biomed. Mater. Res. 2002, 61 (4), 514–523.
(13) Singh, A.; Corvelli, M.; Unterman, S. A.; Wepasnick, K. A.; McDonnell, P.; Elisseeff, J. H. Nat. Mater. 2014, 13 (10), 988–995.
(14) Morgese, G.; Cavalli, E.; Müller, M.; Zenobi-Wong, M.; Benetti, E. M. ACS Nano 2017, 11 (3), 2794–2804.
(15) Sun, Z.; Feeney, E.; Guan, Y.; Cook, S. G.; Gourdon, D.; Bonassar, L. J.; Putnam, D. Proc. Natl. Acad. Sci. U. S. A. 2019, 116 (25), 12437–12441.
(16) Greene, G. W.; Banquy, X.; Lee, D. W.; Lowrey, D. D.; Yu, J.; Israelachvili, J. N. Proc. Natl. Acad. Sci. 2011, 108 (13), 5255–5259.
(17) Neto, A. I.; Vasconcelos, N. L.; Oliveira, S. M.; Ruiz-Molina, D.; Mano, J. F. Adv. Funct. Mater. 2016, 26 (16), 2745–2755.
(18) Kim, K.; Kim, K.; Ryu, J. H.; Lee, H. Biomaterials 2015, 52 (1), 161–170.
(19) Lee, H.; Lee, Y.; Statz, A. R.; Rho, J.; Park, T. G.; Messersmith, P. B. Adv. Mater. 2008, 20 (9), 1619–1623.
(20) Kim, K.; Ryu, J. H.; Lee, D. Y.; Lee, H. Biomater. Sci. 2013, 1 (7), 783.
(21) Swann, D. A.; Bloch, K. J.; Swindell, D.; Shore, E. Arthritis Rheum. 1984, 27 (5), 552–556.
(22) Majd, S. E.; Rizqy, A. I.; Kaper, H. J.; Schmidt, T. A.; Kuijer, R.; Sharma, P. K. Colloids Surfaces B Biointerfaces 2017, 155, 294–303.
(23) Rouxhet, P. G.; Genet, M. J. Surf. Interface Anal. 2011, 43 (12), 1453–1470.
(24) Veeregowda, D. H.; Kolbe, A.; Van Der Mei, H. C.; Busscher, H. J.; Herrmann, A.; Sharma, P. K. Adv. Mater. 2013, 25 (25), 3426–3431.

(25) Tatematsu, M.; Katsuyama, T.; Fukushima, S.; Takahashi, M.; Shirai, T.; Ito, N.; Nasu, T. J. Natl. Cancer Inst. 1980, 64 (4), 835–843.
(26) NIH ImageJ. ImageJ Image processing and analysis in java.
(27) Lattouf, R.; Younes, R.; Lutomski, D.; Naaman, N.; Godeau, G.; Senni, K.; Changotade, S. J. Histochem. Cytochem. 2014, 62 (10), 751–758.
(28) Bulstra, S. K.; Kuijer, R.; Buurman, W. A.; Terwindt-Rouwenhorst, E.; Guelen, P. J.; van der Linden, A. J. Clin. Orthop. Relat. Res. 1992, No. 277, 289–296.
(29) Zappone, B.; Ruths, M.; Greene, G. W.; Jay, G. D.; Israelachvili, J. N. Biophys. J. 2007, 92 (5), 1693–1708.
(30) Neto, A. I.; Cibrão, A. C.; Correia, C. R.; Carvalho, R. R.; Luz, G. M.; Ferrer, G. G.; Botelho, G.; Picart, C.; Alves, N. M.; Mano, J. F. Small 2014, 10 (12), 2459–2469.
(31) Song, L. Nanoscopic vibrations by bacteria adhering to surfaces; 2015.
(32) McNary, S. M.; Athanasiou, K. A.; Reddi, A. H. Tissue Eng. Part B. Rev. 2012, 18 (2), 88–100.
(33) Benz, M.; Chen, N.; Israelachvili, J. J. Biomed. Mater. Res. - Part A 2004, 71 (1), 6–15.
(34) Hong, S.; Yang, K.; Kang, B.; Lee, C.; Song, I. T.; Byun, E.; Park, K. I.; Cho, S. W.; Lee, H. Adv. Funct. Mater. 2013, 23 (14), 1774–1780.
(35) Sivan, S.; Schroeder, A.; Verberne, G.; Merkher, Y.; Diminsky, D.; Priev, A.; Maroudas, A.; Halperin, G.; Nitzan, D.; Etsion, I.; Barenholz, Y. Langmuir 2010, 26 (2), 1107–1116.
(36) Rojas, F. P.; Batista, M. A.; Lindburg, C. A.; Dean, D.; Grodzinsky, A. J.; Ortiz, C.; Han, L. 2015.
(37) Han, L.; Grodzinsky, A. J.; Ortiz, C. Annu. Rev. Mater. Res. 2011, 41 (1), 133–168.
(38) Peng, G.; McNary, S. M.; Athanasiou, K. A.; Reddi, A. H. Cartilage 2016, 7 (3), 256–264.
(39) Pritzker, K. P. H.; Gay, S.; Jimenez, S. A.; Ostergaard, K.; Pelletier, J. P.; Revell, K.; Salter, D.; van den Berg, W. B. Osteoarthr. Cartil. 2006, 14 (1), 13–29.
(40) Li, W.; Shi, L.; Deng, H.; Zhou, Z. Tribol. Lett. 2014, 55 (2), 261–270.
(41) Majd, S. E.; Kuijer, R.; Köwitsch, A.; Groth, T.; Schmidt, T. A.; Sharma, P. K. Langmuir 2014, 30 (48), 14566–14572.
(42) Lopata, A. L.; O'Hehir, R. E.; Lehrer, S. B. Clin. Exp. Allergy 2010, 40 (6), 850–858.
(43) Ghormade, V.; Pathan, E. K.; Deshpande, M. V. Int. J. Biol. Macromol. 2017, 104, 1415–1421.
(44) Pu, J.; Jiang, D.; Mo, Y.; Wang, L.; Xue, Q. Surf. Coatings Technol. 2011, 205 (20), 4855–4863.
(45) You, A.; Be, M. A. Y.; In, I. 2007, 093702.
(46) Pettersson, T.; Dėdinaitė, A. J. Colloid Interface Sci. 2008, 324 (1–2), 246–256.
(47) Ducker, W. A.; Senden, T. J.; Pashley, R. M. Nature 1991, 353 (6341), 239.
(48) Pettersson, T.; Nordgren, N.; Rutland, M. W.; Feiler, A. Rev. Sci. Instrum. 2007, 78 (9), 93702.
(49) Bogdanovic, G.; Meurk, A.; Rutland, M. W. 2000, 19, 397–405.
(50) Kuijer, R.; Emans, P.; Jansen, E.; Hulsbosch, M.; Surtel, D.; Bulstra, S. In 49th Annual Meeting of the Orthopaedic Research Society Paper # 0101; 2003; Vol. 67, p 101.

(51) Huang, X.; Bao, X.; Liu, Y.; Wang, Z.; Hu, Q. Sci. Rep. 2017, 7 (1), 1–10.
(52) Singh, A.; Zhan, J.; Ye, Z.; Elisseeff, J. H. Adv. Funct. Mater. 2013, 23 (5), 575–582.
(53) Zhou, Q.; Kühn, P. T.; Huisman, T.; Nieboer, E.; Van Zwol, C.; Van Kooten, T. G.; Van Rijn, P. Sci. Rep. 2015, 5 (November), 1–12.

Supporting information

Materials and Methods

Synthesis of and characterization of chitosan-catechol (Chi-C). Chi-C was synthesized through the EDC reaction between the carboxyl group from hydrocaffeic acid and the amine group from chitosan [20] at pH 5 (Figure 1). Briefly, Chitosan (50kDa-190kDa, 3.25 mmol, Sigma Aldrich, CAS no. 9012-76-4) was dissolved in 50 ml PBS and pH was adjusted to 5 by 1N HCl and 1N NaOH solutions. Hydrocaffeic acid (HCA, 3.25 mmol, Sigma Aaldrich, CAS no. 1078-61-1) dissolved in 1 ml of deionized water was then added to the chitosan solution. EDC (3.25 mmol, Sigma Aaldrich, CAS no. 25952-53-8) and N-Hydroxysuccinimide(NHS, 3.25 mmol, Sigma Aaldrich, CAS no. 6066-82-6) predissolved in 2mL of deionized water and ethanol (Sigma Aaldrich, CAS no.64-17-5) solution (1:1, v/v) was added to the reaction mixture, which was stirred at room temperature in a nitrogen environment. The pH of the reaction was checked every 20 min and readjusted if necessary. After 9 h, the mixture compound was dialyzed (molecular weight cut-off: 3500 Da, spectrum medical industries, USA) in acidified deionized water (pH 5.0) for 2 days. The final product was lyophilized and stored in a moisture-free desiccator.

The conjugation property was determined by using ^{1}H-NMR (Avance, Bruker Inc., USA,) with a concentration of 5mg/ml in D_2O and in the FTIR (Agilent technologies, Santa Clara, USA) as a powder. The degree of catechol substitution was determined using a Uv-Vis (Beckman, USA) spectrum at 280 nm with the standard hydrocaffeic acid curve as follows: hydrocaffeic acid solutions with concentrations ranging from 0.1mM to 0.9 mM in PBS were prepared and their absorbance at 280 nm was measured by Uv-Vis spectrum. The calibration curve thus obtained is presented in Figure S1. After obtaining the absorbance of 1 mg/ml Chi-C at 280nm, the conjugate degree was calculated by using the calibration curve. For all the experiments Chi-C was dissolved in PBS (pH 7) at a concentration of 10 mM.

Colloidal probe atomic force microscopy for studying lubrication at nanoscale[24]. Rectangular, tipless cantilevers (length 300±5um, width 35±3um) were calibrated for their torsional and normal stiffness by the thermal noise

method[45] using AFM Tune IT v2.5 software [46,47]. The normal stiffness (K_n) was between 0.01 and 0.05 N/m and the torsional stiffness (K_t) between 1 and 4×10^{-9} Nm/rad. A silica particle 21.83 µm in diameter (Bangs laboratories, Fishers, IN, USA) was glued to a cantilever with epoxy glue (Pattex, Brussels, Belgium). The deflection sensitivity (α) of the colloidal probe was recorded at a constant compliance with bare crystal in buffer to calculate the normal force (F_n) applied using

$$F_n = \Delta V_n * \alpha * K_n \quad (1)$$

where ΔV_n is the voltage output from the AFM photodiode due to normal deflection of the colloidal probe. The torsional stiffness and geometrical parameters of the probe were used to calculate the friction force (F_f) [48] according to

$$F_f = (\Delta V_L * K_t) / 2\delta * (d + t/2) \quad (2)$$

where t is the thickness of the cantilever, δ is the torsional detector sensitivity of the AFM calculated by a standard torsional photodetector calibration[45,49]. Briefly δ is calculated by using a mirror on the base of the AFM for reflection of the laser in to the detector. The lateral detector voltage was recorded as the mirror was tilted over several angles. From the lateral detector voltage against the tilt angle (rad) the δ (v/rad) can be calculated for the used medium (air/liquid). The detector signals both normal and torsional were grabbed with a DAQ card from National Instruments. ΔV_L corresponds to the voltage output from the AFM photodiode due to lateral deflection of the probe. Lateral deflection was observed at a scanning angle of 90 degrees over a scan line of 10 µm and a scanning frequency of 1 Hz.

The colloidal probe was incrementally loaded up to a normal force of 40 nN. At each normal force, friction loops were recorded to yield the average friction force. Finally, the coefficient friction was taken as the slope of a straight line fitted to the friction vs. normal force data. The surface softness was measured by colloidal probe AFM and by repulsive force-distance curve measurement. The repulsive force-distance curves between the colloidal probe and adsorbed film were obtained at a trigger threshold force of 10 nN. Assuming the stiffness and Poisson's ratio for Au and SiO_2 to be 80, 200 GPa and 0.4, 0.3 respectively the applied normal force would give rise to contact pressures of 4-43 MPa.

Evaluation of cell behavior. Cell response to Chi-C treated S-SyCF was tested on chondrocytes derived from human cartilage [28,50] using a protocol described in detail in the supplementary information. were seeded onto 15 mm (15mm ϕ) circular glass slides that fit into the 24-well culture plate. The circular slides were dipped in synovial fluid for 30 min and immersed in PBS or Chi-C (0.5 mg/ml in PBS) for 10 min and for another 30 min in synovial fluid (the same procedure used for QCM-D experiment). Control glass slides were dipped only in PBS. Each sample was sterilized by UV radiation for 1 h and seeded with cells at a concentration of 5×10^3 cells/ml. Cells were cultured in a high glucose DMEM (Gibco), 10% FBS (Gibco), and 1% penicillin–streptomycin (Sigma) at pH 7.4 and incubated at 37°C in a humidified air atmosphere of 5% CO_2 ; the medium was changed every 3 to 4 days. Cell viability and proliferation were measured by using an XTT assay (Applichem A8088), which is briefly summarized as follows. On day 1, day 3, day 7 and day 14, 300ul of XTT reaction reagent (0.1 ml activation reagent and 5 ml XTT mixture) was added to each well and incubated at 37°C for 3 h. The microplate reader was used to record absorbance at 485 and 690 nm. Fluorescent images using confocal laser scanning microscopy (CLSM) with TRITC-phalloidin and DAPI stain showed the visual morphology of chondrocytes. Cells were fixed by paraformaldehyde for 15 min at room temperature, followed by washing with PBS, then 500 ul mixture (TRITC-labelled phalloidin at 2 ug/ml and DAPI 4ug/ml in PBS) was added to each well plate, which was then incubated for 1 h at room temperature with aluminum foil for light protection. The mixture was then removed, washed with PBS and visualized by CLSM.

Results

Synthesis and characterization of chitosan catechol (Chi-C) polymer.

The H-NMR spectra of Chi-C obtained through the EDC reaction (post dialysis) is shown in Figure S1b. The multiplets observed between δ = 6.5 ppm and δ = 7.0 ppm are associated with protons of the catechol; the region around 2 ppm corresponds to protons from the acetyl group, demonstrating that Chi-C conjugation was successful. The conjugation was also confirmed using FTIR spectra shown in FigureS1c, where new absorption peaks around 1289 cm^{-1} correspond to the characteristic absorption of phenolic structures. The

adsorption peaks at 1530 cm^{-1} (amide type II) also increased in intensity, suggesting that the amine group on chitosan reacted with the carboxyl from hydrocaffiec acid to form amide linkage (CO-NH) [51]. In the UV-Vis spectroscopy spectra (Figure S1d) the Chi-C conjugate can also be clearly observed in the absorption at 280 nm from aromatic nucleus, which is not observed for chitosan alone. The conjugation level was calculated with the standard curve of hydrocaffeic acid using the absorbance at 280 nm with different concentrations (see Figure S2). After obtaining the absorbance of 1 mg/ml (5.4 mM) Chi-C at 280nm, the conjugation degree can be calculated. In the present study, 1mg/ml product absorbance at 280 nm was 1.83 (0.689 mM), thus indicating that a 12.7% conjugation level for Chi-C was achieved and the molecular weight of Chi-C would be 55.2 to 209.8 kDa. Amidation by the carbodiimide coupling method [30] is widely used in biomaterial applications due to its eco-friendly nature and high yield. Different proportions between chitosan and hydrocaffeic acid can yield different conjugations. In the present study, we chose a 12.7% conjugation level because less than 10% is conventionally considered to be a low catechol conjugation level for a polymer. Likewise, conjugation above 25% is regarded as high catechol conjugation level for a polymer because such higher levels are limited by aggregate formation during the EDC reaction [18,52].

Biocompatibility of Chi-C

In terms of the specific location of sliding as it naturally occurs, it is necessary to check the biocompatibility of SyCF after modification with Chi-C. We therefore co-cultured the S-SyCF (after modification with Chi-C) with human chondrocyte cells for 2 weeks. After 1, 3, 7 and 14 days, the cells were analyzed by confocal microscopy and XTT viability assays (see FigureS4). The overview images on each surface clearly display more cell surface coverage after 7 days compared to 1 and 3 days, although no significant difference was found in metabolic activity between the different surfaces. The numbers of nuclei per mm^2 on each surface in FigureS4c increased gradually with culture time, indicating that cell proliferation on each surface was not affected by the surface chemistry during this short period. Moreover, on day 14, cell proliferation and metabolic activity were significantly higher on S-SyCF with

Chi-C than on S-SyCF with PBS and on bare glass. This difference could be due to the presence of a soft and highly hydrated S-SyCF. Chi-C treatment gives rise to a thicker (Figure 1c) and softer (Figure 1d) S-SyCF than with buffer treatment, although no significant difference was observed with respect to the metabolic activity between them. Stiffness of the substrate upon which the cells find themselves has a clear effect on their morphology and activity [53]. The above result indicates that the proliferation of chondrocytes *in vitro* in the long term (after two weeks) could be affected by the surface chemistry as well as by the structure softness. As the time increased, more and more cells appeared on the surface (see FigureS4a). The average number of cells first increased until day 7 and then decreased gradually on day 14 (see FigureS4c), which could be caused by the limited space for each cell with the increasing numbers of cells. Both microscopic examination and XTT assay showed that S-SyCF with Chi-C treatment enables human chondrocyte cells to be as active metabolically and to proliferate and spread as rapidly as S-SyCF with buffer treatment.

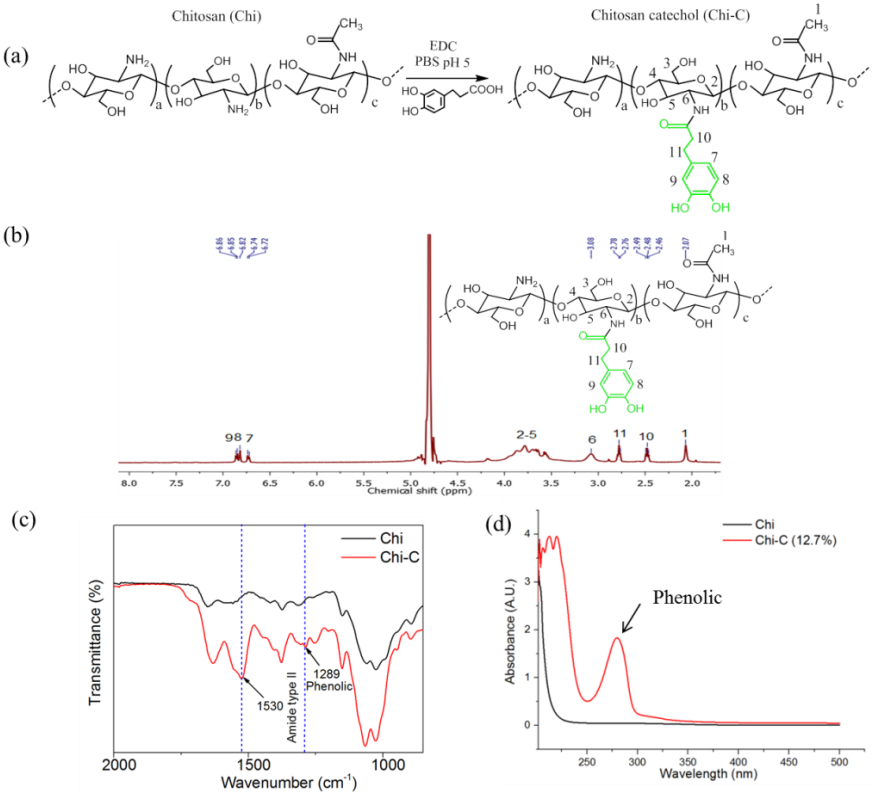

Figure S1. Synthesis and characterization of Chi-C (a) Synthesis and chemical structure of Chi-C. (b) ^{1} H-NMR spectra of Chi-C. (c) FTIR spectrum of Chi and Chi-C. (d) UV-Vis spectra of Chi-C and the control (Chi).

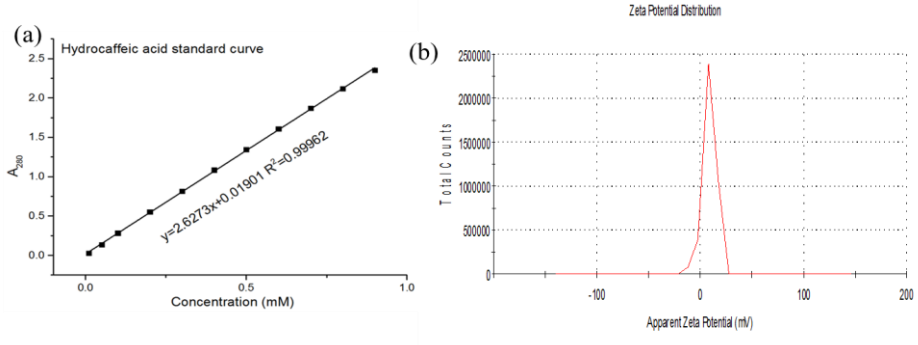

Figure S2. Uv-Vis spectra of hydrocaffeic acid solution at A_{280} with concentrations ranging from 0.1mM to 0.9mM, and the standard curve (a) calculated by the linear fitting. (b) Zeta potential of Chi-C at 0.5mg/ml in PBS.

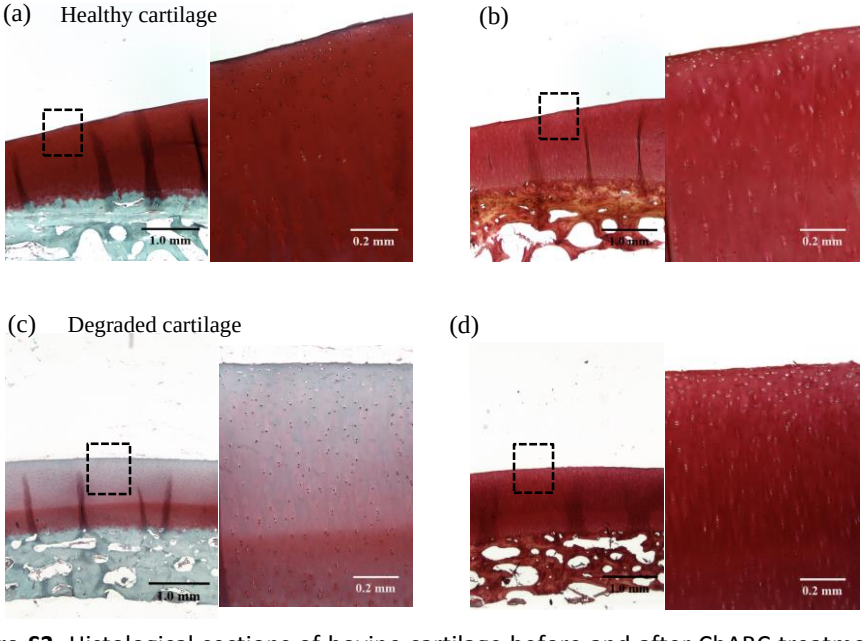

Figure S3. Histological sections of bovine cartilage before and after ChABC treatment. (a) Histology sections of cartilage without ChABC treatment were stained with Safranine-O with Fast Green for proteoglycans and GAGs. (b) Sections of cartilage without ChABC treatment were stained with Picrosirius red for collagen. (c) and (d) show the cartilage degraded by ChABC, which were stained with Safranine-O with Fast

Green for proteoglycans and GAGs and Picrosirius red for collagen, respectively. The images were taken at magnifications of 2.5× and 10×. The black square indicates the enlarged area.

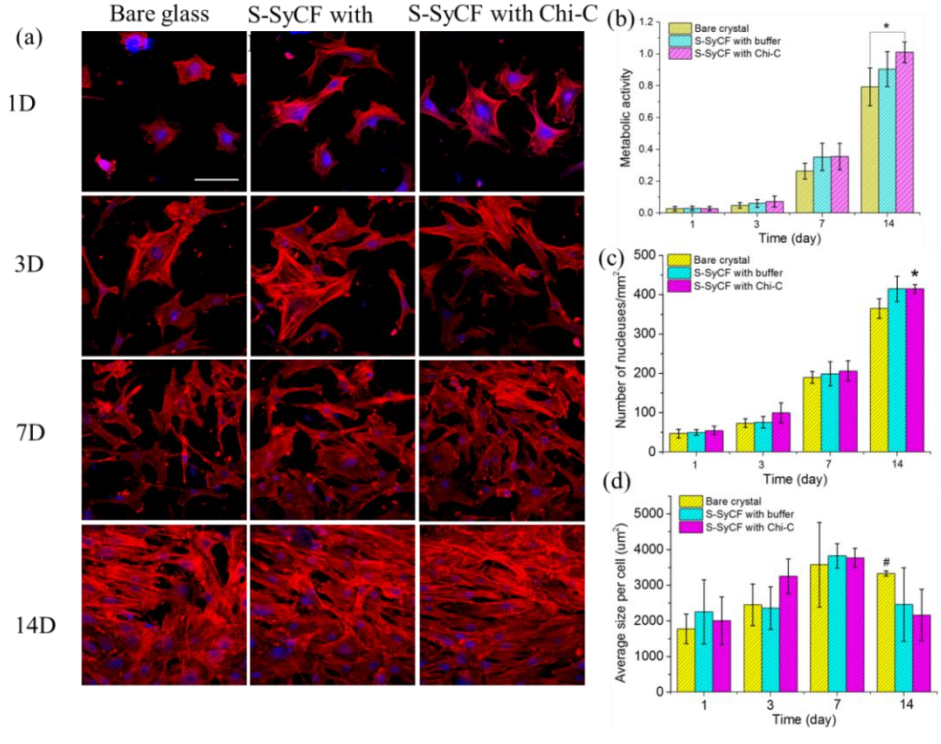

Figure S4. Behavior of chondrocyte cells on different surfaces. (a) Fluorescence images of cells stained with DAPI (nucleus) and TRITC-pholloaid (cytoskeleton) for Chondrocyte cells at 1, 3, 7 and 14 days of culture. (b) XTT assay shows an increasing trend in metabolic activity, which is dependent on both cell viability and proliferation for each surface. (c) Numbers of nuclei per mm^2 on different surfaces. (d) Average size per cell on different surfaces at different culture times. * Statistically significant $p < 0.05$ (two-tailed Student t-test) differences of cell metabolic activity and numbers of nucleuses at 14 days on S-SyCF with Chi-C compared to bare glass. # Statistically significant differences of average size per cell on cell at 14 days on bare glass compare to S-SyCF with Chi-C. Scale bare in the image represents 100 um.

Table S1. Surfaces elemental composition of SF with PBS and SF with Chi-C

%	S-SyCF exposed to buffer		S-SyCF exposed to Chi-C
C	60.4±2.1		59.8±0.02
O	O_{total}	18.6±1.1	19.87±0.04
	$\%O_{532.7}*O_{total}$	4.8±0.3	5.86±0.25
N	11.2±0.36		10.5±0.33
P	2.4±0.5		2.55±0.02
S	1.06±0.03		0.93±0.45
Cl	3.5±0.28		3.46±0.14
Na	2.9±0.3		2.72±0.45